Progress In Electromagnetics Research C, Vol. 110, 81–89, 2021

Gain Flattening of Wideband FPC Antenna Using Elliptical and Rectangular Slotted AMC Layers

Nayana Chaskar[1], Shishir D. Jagtap[1], Rajashree Thakare[2], and Rajiv K. Gupta[1, *]

Abstract—In this paper, the gain flattening of a wideband Fabry-Perot cavity (FPC) antenna, using truncated partially reflecting surface (PRS) and slotted elliptical and rectangular shape artificial magnetic conductor (AMC) layers is proposed. FPC is fed using a metal plated microstrip antenna (MSA) which comprises three layers — elliptical slotted rectangular AMC-I layer, truncated PRS layer, and rectangular slotted elliptical AMC-II layer. AMC-II layer is designed complementary to AMC-I layer to obtain gain variation < 1 dB over wide frequency band. Elliptical shaped AMC-II and truncated PRS reduce the reflected fields towards ground and thus improve front to back lobe ratio (F/B) and side lobe level (SLL). These layers resonate at higher frequency and thus reduce gain variation and couple electromagnetically with MSA and AMC-I layer to provide wide bandwidth (BW). The proposed antenna provides $S_{11} < -10$ dB, 17.2 dBi peak gain with gain variation < 1.2 dB over 5.7–6.4 GHz frequency band, which covers 5.725–5.875 GHz ISM and 5.9–6.4 GHz satellite uplink C band. Broadside radiation patterns have SLL < -19 dB, cross polarization (CPL) < -17 dB, and F/B > 20 dB with wide 3 dB gain BW of 15.2%. The overall antenna dimensions are $2.3\lambda_0 \times 2.75\lambda_0 \times 0.5\lambda_0$, where λ_0 is the free space wavelength corresponding to 5.8 GHz, central frequency of ISM frequency band. The measured results of the prototype fabricated structure agree with simulation ones.

1. INTRODUCTION

Recently, various techniques have been reported to enhance the gain BW of FPC antennas. High gain wide band FPC antennas should offer advantages like ease of fabrication, simple feeding technique, low cost, and improved radiation characteristics viz. low CPL, low SLL, and low gain variation over wide band. Hence, high impedance surface (HIS), frequency selective surface (FSS), reactive impedance surface (RIS), partially reflected surface (PRS), artificial magnetic conductor (AMC), and electromagnetic band gap (EBG) structures have attracted significant attention in the design of wideband FPC antennas [1–17].

The printed compound air-fed array antenna, with a flat gain-frequency response is designed, using FSS cover and inversely tapered mushroom type HIS in FPC [1]. These techniques enlarge the gain-BW product and improve the aperture efficiency of the antenna. A broadband, low profile, wideband MSA array, sandwiched between RIS and PRS layers has been reported in [2]. The RIS and PRS consist of an array of square patches of dimension and periodicity much smaller than the wavelength. The PRS in FPC antenna is designed by fabricating parasitic metallic patches on a superstrate layer to enhance the gain of the primary radiator. Various PRS structures are designed using single layer [3, 4], dual layer [5], and triple layer [6] superstrates and analysed for gain enhancement.

Frequency selective surfaces (FSS) are periodic structures used to reflect, transmit, or absorb electromagnetic waves. Various FSS structures are designed in [7–9], as a class of wideband PRS,

Received 4 January 2021, Accepted 15 February 2021, Scheduled 20 February 2021
* Corresponding author: Rajiv Kumar Gupta (rajivmind@gmail.com).
[1] Department of Electronics and Telecommunication, Terna Engineering College, Navi-Mumbai, India. [2] Bharti Vidhyapeth College of Engineering, Navi-Mumbai, India.

which exhibit frequency filtering properties. Directivity enhancement of EBG antenna with single FSS layer [7], wideband Fabry-Perot resonator antenna (FPRA) with two complementary FSS layers [8], and dual band FPC antenna with shared-aperture FSS layer [9] have been reported.

A compact high gain resonant cavity antenna (RCA) with via hole feed patch and hybrid parasitic ring superstrate is designed in [10]. Various FPC antennas based on different techniques such as shaped ground plane [11], modified AMC-PRS layers [12], and stratified meta-surfaces [13] have been investigated. A dual-wideband high-gain antenna is reported in [14] while a wideband FPRA is designed with two layers of electrically thin dielectric superstrates in [15]. An orthogonally polarized high gain antenna, using double layer of Jerusalem-Cross PRS [16] and a dual-band frequency reconfigurable PRS with PIN diodes [17] have been reported. However, these antennas suffer from high SLL and small gain BW product.

Besides complex feeding technique, high SLL and gain variation have been observed over wide frequency band in reported antennas. To overcome these limitations, a high gain wideband FPC antenna by using elliptical and rectangular slotted AMCs and truncated PRS layer is designed. An elliptical AMC layer reduces the reflected fields towards the ground and thus improves F/B ratio. The AMC-PRS layers are modified to resonate, at higher frequencies to increase gain at higher frequencies and to provide flat gain-frequency response over wide BW. The proposed antenna is compact, light weight, low cost, and easy to fabricate. It offers 17.2 dB peak gain, 15.2% gain BW, SLL < -19 dB, CPL < -17 dB, and gain variation < 1.2 dB over 5.7–6.4 GHz frequency band.

2. ANTENNA GEOMETRY AND DESIGN THEORY

The proposed antenna comprises metal plated MSA, AMC-I, PRS, and AMC-II. The side view of the proposed antenna is shown in Fig. 1(a), while the top views of AMC-I, AMC-II, and truncated PRS are shown in Figs. 1(b)–(e). A 0.5 mm thick, rectangular copper metal plated MSA is suspended at 1.8 mm above the ground plane. The rectangular AMC-I is designed, using an array of 4 mm square metallic patches, with inter-element spacing of 1 mm and printed on the bottom side of 1.59 mm thick, FR4 superstrate-I [2].

A rectangular AMC-I, with elliptical shaped slot, as shown in Fig. 1(b), is placed at 0.48 mm above the MSA, and superstrate-II is placed at about $0.5\lambda_0$ from feed patch to form FPC. Elliptical slotted AMC-I improves the bandwidth of antenna. Truncated PRS, as shown in Fig. 1(e), is formed using square patches, with side dimension about 0.5λ, spaced at about 1λ, and printed on the bottom side of superstrate-II, where λ is the wavelength in dielectric at 5.8 GHz. An elliptical AMC-II, with a rectangular slot, as shown in Fig. 1(d), is fabricated on the other side of superstrate-II. The dielectric constant and loss tangent of FR4 superstrates are 4.4 and 0.02, respectively. The antenna structure is fed by a 50 Ω coaxial probe. The structures are simulated using method of moment based IE3D 14.0 simulator.

An FPC antenna is a cavity resonator antenna consisting of a PRS and a perfectly reflecting ground plane. FPC is fed by an MSA. FPC antenna has high gain and narrow BW, when all the elements that constitute the FPC resonate in unison. However, when different elements of FPC resonate at different but nearby frequencies, the resonant cavity resonates at two or more nearby frequencies, which electromagnetically couple to provide wide impedance and gain BW. The resonant frequency of an FPC antenna depends on feed antenna dimensions, height of FPC, and dimensions and spacing of parasitic patches fabricated on an FR4 superstrate, which acts as a PRS in the proposed antenna. The gain at lower frequencies can be increased by increasing the dimensions of one or more elements or height of FPC and vice-versa. Thus different elements can be optimized to enhance the gain BW of FPC antenna. A wide gain FPC antenna should have a wideband feed antenna.

Wide gain BW in the proposed antenna is obtained by enhancing the BW of feed antenna. To obtain broad impedance BW, a metal plated rectangular suspended MSA with air as a dielectric is designed to feed the FPC. An AMC-I layer with an elliptical slot is placed above it, and the dimensions of MSA and AMC-I with an elliptical slot are optimized. The AMC layer has its own resonant frequency, which depends on the dimension of square patches, spacing between the patches, and the distance between ground and AMC layers. In slotted AMC, the removal of patches decreases the effective capacitance and inductance of AMC, and therefore, it resonates at higher frequency. Since there is gradual variation

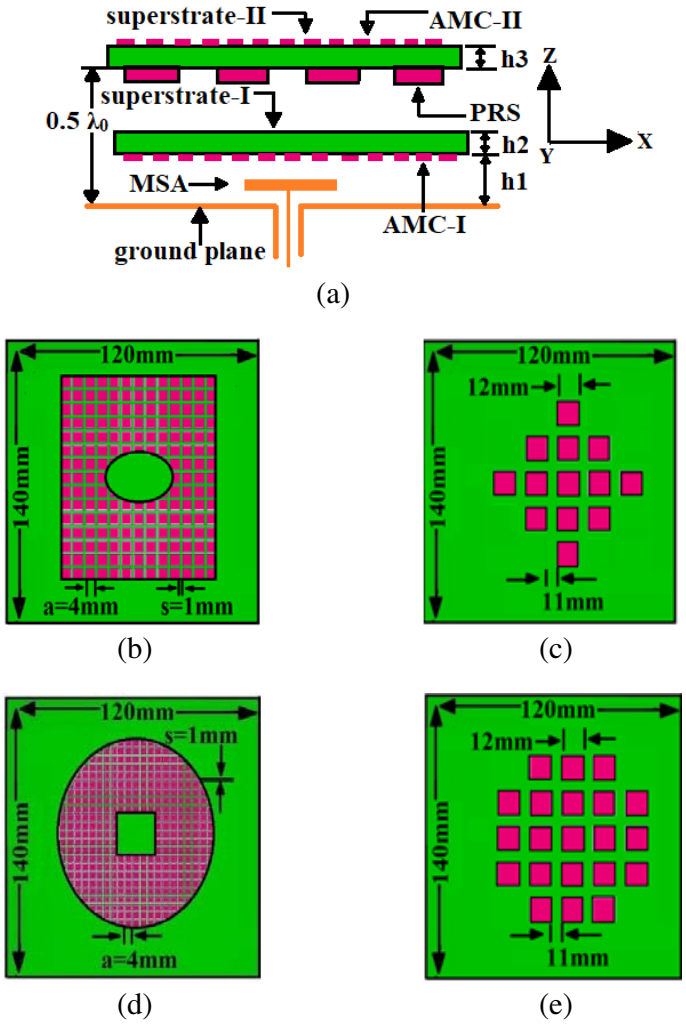

Figure 1. Geometry of proposed antenna (Center of all layers and ground plane are aligned). (a) Side view (AMCs and PRS are truncated and should be seen with its top view), (b) AMC-I, (c) truncated PRS, (d) AMC-II, (e) truncated PRS.

of inductance and capacitance in AMC-I with an elliptical slot, it provides larger impedance BW than a rectangular, square, or circular slot [12, 18]. The periodic structure used on the superstrate is merely an FSS. However, the reflection phase variation of the unit cell is within $\pm 90°$, over the operating frequency band, and therefore, it is termed as AMC [12].

The gain of an FPC antenna depends on the feed antenna and reflection coefficient of PRS. Metallic patches are good reflector of electromagnetic waves and thus increase the reflection coefficient and gain of the antenna. Therefore, gain of the proposed FPC depends on PRS and AMC-II layer [12]. Corner truncated PRS has effectively smaller dimensions than PRS without any truncation and thus improves the gain of the antenna at higher frequencies. Since the width of MSA is more than its length, an elliptical AMC-II is designed so that it can provide higher gain. An elliptical AMC-II offers lower SLL and larger gain BW than rectangular AMC-II. A rectangular AMC-II has higher SLL, due to reflection at the sharp corner of rectangular AMC-II. A square or circular AMC-II offers lower gain and slightly higher SLL and CPL.

AMC-II surface is designed complementary to AMC-I surface, so as to decrease SLL, CPL, and gain variation over wide frequency band. PRS with truncated corner also increases the gain at higher frequency and thus reduces gain variation. Truncated PRS and elliptical AMC-II reduce the reflected fields towards ground and thus improve F/B lobe ratio. As the electric field coupling along X-axis is

more than Y-axis, an elliptical AMC-II provides higher gain with low SLL than circular or rectangular or square AMC. The dimensions of metal plated MSA, AMC-I, PRS, AMC-II, FPC height and AMC-I layer height are optimized to obtain wide gain BW (15.2%) with < 1.2 dB gain variation over frequency band 5.7–6.4 GHz. The proposed antenna operates over 5.7 GHz to 6.62 GHz with 6.16 GHz as central operating frequency. The optimum dimensions of the proposed antenna are listed in Table 1. All dimensions are in mm only.

Table 1. Dimensions of proposed antenna.

Ground plane length × width	120 × 140	Square patch dimensions of AMC-I and AMC-II	4
MSA length × width	18.6 × 21.3	Spacing between square patches of AMC-I and AMC-II	1
Feed position of MSA from centre along x axis	7	Square patch dimensions of PRS	12
AMC-I length × width	64 × 74	Spacing between square patches of PRS	11
major and minor length of elliptical slot of AMC-I	28 × 18	Height of MSA from ground	1.8
major and minor length of elliptical AMC-II	114 × 104	Height of AMC-I from ground	2.3
Slot length × width in AMC-II	26 × 26	Height of PRS from ground	27

3. SIMULATION RESULTS AND ANALYSIS

Initially, a metal plated MSA is suspended at a height of 1.8 mm above the ground plane, and a rectangular uniform AMC-I, without any slot, is printed on the bottom side of superstrate-I. The MSA is fed using a 50 Ω coaxial probe at 3.8 mm from the center of MSA, along X-axis. AMC-I increases the L and C of structure and as a result, decreases the resonant frequency. An ellipse shape slot is introduced in the uniform AMC-I layer, by removing patches from its center, as shown in Fig. 1(b). Slotted AMC-I resonates at higher frequency than uniform AMC-I, since removal of patches reduces L and C of the structure.

Now the MSA along with an ellipse shape slotted AMC-I is placed in FPC to enhance the gain of the antenna. The PRS layer is placed at about $0.5\lambda_0$ height from the ground plane, as shown in Fig. 1(a). A PRS is formed by printing square patches of size 12 mm and periodicity 23 mm on an FR4 superstrate. FPC antenna gain depends on the reflection coefficient of the PRS layer [12]. Antenna gain increases with patches on the PRS as it increases the reflection coefficient of PRS. The proposed antenna is designed with truncated PRS as shown Fig. 1(e). As truncated PRS has smaller dimensions, it increases the gain at higher frequencies and decreases gain variation. Besides this, corner patches in non-truncated PRS increase SLL; therefore, truncated PRS also improves SLL.

Now, a rectangular slotted elliptical AMC-II layer, as shown in Fig. 1(d), is designed using an array of square metallic patches of side 4 mm and inter element spacing of 1 mm and printed on the upper side of FR4 superstrate-II. AMC-II layer is designed complementary to AMC-I, to reduce SLL, CPL, and gain variation. The addition of AMC-II not only increases the gain BW but also increases effective reflection coefficient of the PRS layer, which in turn increases the antenna gain. The structure with AMC-I, single patch on PRS and AMC-II is termed as ANT1.

The optimized 'ANT.1' provides a peak gain of 14.5 dB, SLL < -21.1 dB, CPL < -17.4 dB, F/B ratio > 21.2 dB, and $S_{11} < -10$ dB over 5.7 GHz to 6.5 GHz frequency band. The overall size of 'ANT.1' is $1.7\lambda_0 \times 2.1\lambda_0$. The 'ANT1' with AMC-II layer reduces the SLL and CPL significantly, as compared to 'ANT.1' without AMC-II layer.

The antenna gain is enhanced further by increasing the size of PRS array. Thereafter, a 2×2 array of square metallic patches of side 12 mm and inter element spacing of 11 mm is placed at PRS layer with AMC-II layer, and this structure is termed as 'ANT.2'. These 2×2 patches act as a space fed array antenna. Therefore, the dimensions and periodicity of PRS patches are larger than the metallic patches on AMC-I and AMC-II layers. Similarly, 'ANT.3' with a 3×3 PRS array is designed and optimized. S_{11} and gain variation of these structures are shown in Fig. 2.

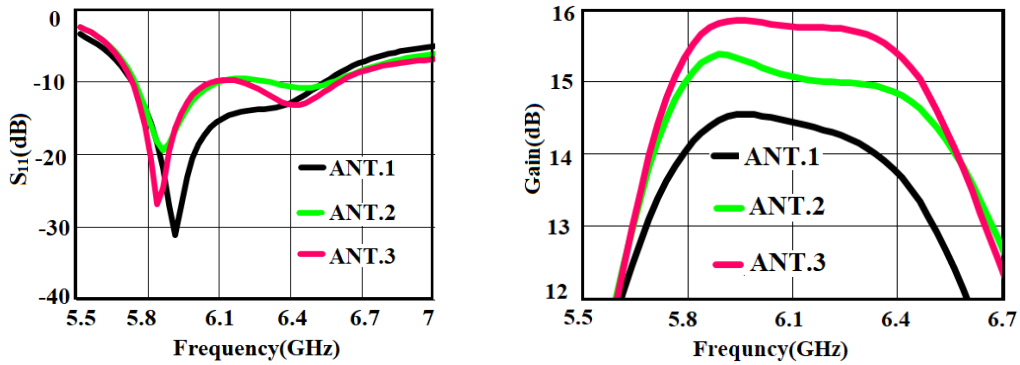

Figure 2. (a) S_{11} vs. frequency, (b) gain vs. frequency.

4. GAIN BANDWIDTH ENHANCEMENT

The PRS array size is further increased to achieve wide gain BW. The 'ANT.4' with truncated PRS-I, as shown in Fig. 1(c), is designed and optimized. The optimized 'ANT.4' provides a peak gain of 16.6 dBi, SLL < -18.7 dB, CPL < -16.3 dB, F/B ratio > 20 dB, and $S_{11} < -10$ dB over 5.7 GHz to 6.6 GHz frequency band. Though the gain of antenna has increased, SLL and CPL have also increased at higher frequencies.

The 'ANT.5' with 4×4 PRS array and 'ANT.6' with 5×5 PRS array are designed and optimized. The optimized 'ANT.5' provides a peak gain of 16.9 dBi, SLL < -18.7 dB, CPL < -17.9 dB, and F/B ratio > 20 dB. The optimized 'ANT.6' provides a peak gain of 17.3 dBi, SLL < -17.9 dB, CPL < -17.2 dB, F/B ratio > 18.3 dB, and $S_{11} < -10$ dB over 5.7 GHz to 6.6 GHz frequency band. Gain increases with the increase in array size, but SLL, CPL also increase, and F/B lobe ratio decreases in ANT.6.

Now, the corner metallic patches are removed from the 5×5 array of PRS layer to form truncated

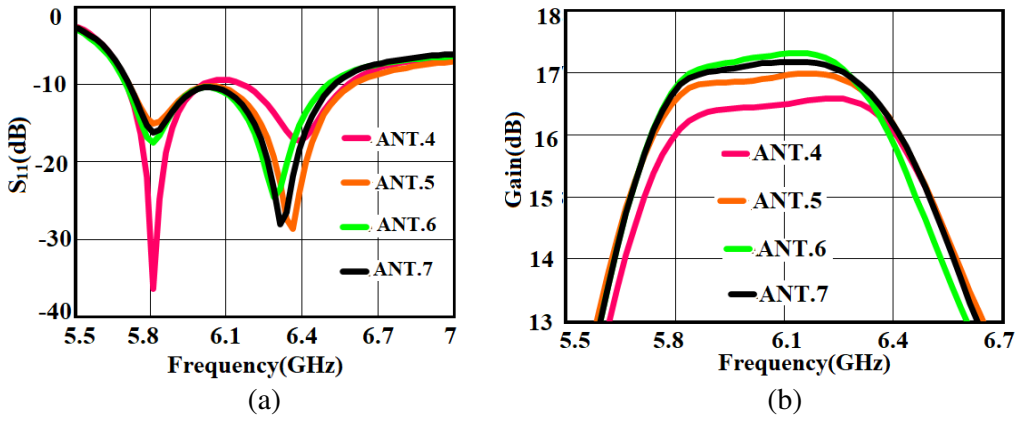

Figure 3. (a) S_{11} vs. frequency, (b) gain vs. frequency.

PRS-II, as shown in Fig. 1(e). This antenna structure termed as 'ANT.7' is optimized. The 'ANT.7' offers flat gain-frequency response with gain variation < 1.2 dB and 3-dB gain BW of 15.2%. This antenna provides peak gain of 17.2 dBi, SLL < -18.6 dB, CPL < -18.0dB, and F/B ratio > 20 dB. All the structures from ANT.1 to ANT.7 depict gain flattening. Peak gain has increased by 2.7 dB from ANT.1 to ANT.7. ANT.1 to ANT.3 have a peak gain less than 16 dBi, while ANT.4 to ANT.7 have a peak gain about 17 dBi. Compared to ANT.6, ANT.7 offers lower SLL and CPL and higher F/B lobe ratio with improved 3 dB gain BW. S_{11} and gain variation of these structures are shown in Fig. 3. The simulated radiation patterns of proposed antenna 'ANT.7' are shown in Fig. 4. The radiation parameters of 'ANT.1' to 'ANT.7' structures at frequency 5.8 GHz and 6.15 GHz are listed in Table 2.

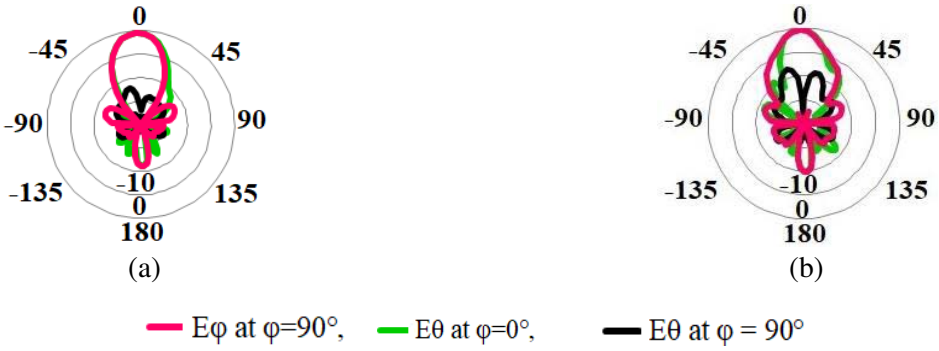

Figure 4. Radiation patterns of ANT. 7 at (a) 5.8 GHz and (b) 6.15 GHz.

Table 2. Radiation parameters.

ANT. Str.	Gain (dBi)	3 dB Gain BW (GHz)	SLL (dB) 5.8|6.15 GHz	CPL (dB) 5.8|6.15 GHz	F/B (dB)	Size (λ_0^2)
1	14.5	1.06	$-22.5\| - 21.1$	$-22.5\| - 17.4$	17.6	1.7×2.1
2	15.4	1.12	$-20.4\| - 19.4$	$-23.7\| - 17.8$	19.6	1.9×2.3
3	15.8	1.04	$-19.2\| - 19.7$	$-23.8\| - 17.4$	23.6	2.1×2.5
4	16.6	0.96	$-23.3\| - 18.7$	$-23.2\| - 16.3$	20.0	2.3×2.7
5	16.9	0.95	$-21.3\| - 18.7$	$-24.0\| - 17.9$	20.0	2.3×2.7
6	17.3	0.86	$-19.6\| - 17.9$	$-24.1\| - 17.2$	18.3	2.3×2.7
7	17.2	0.92	$-22.1\| - 18.6$	$-24.2\| - 18.0$	20.0	2.3×2.7

5. FABRICATION AND MEASUREMENT RESULTS

The fabricated prototype 'ANT.7' structure is shown in Fig. 5. The return loss (S_{11}) is measured by using 9916A Agilent network analyzer. The radiation patterns and gain of the antenna are measured by using a standard horn antenna. The simulated and measured S_{11} and gain variation are shown in Fig. 6. The measured results are in good agreement with the simulation ones. Fabrication error and alignment can be attributed to the discrepancy between simulated and measured results. The measured broadside radiation patterns at 5.8 GHz and 6.15 GHz are shown in Fig. 7.

6. COMPARISON WITH STATE OF ART ANTENNAS

The comparison of the proposed antenna with the existing state of art FPC antennas structures is listed in Table 3. While comparing the different antennas, we have considered peak gain, common bandwidth (common BW include BW which is common to 3 dB gain BW, 10 dB impedance BW and 3 dB axial

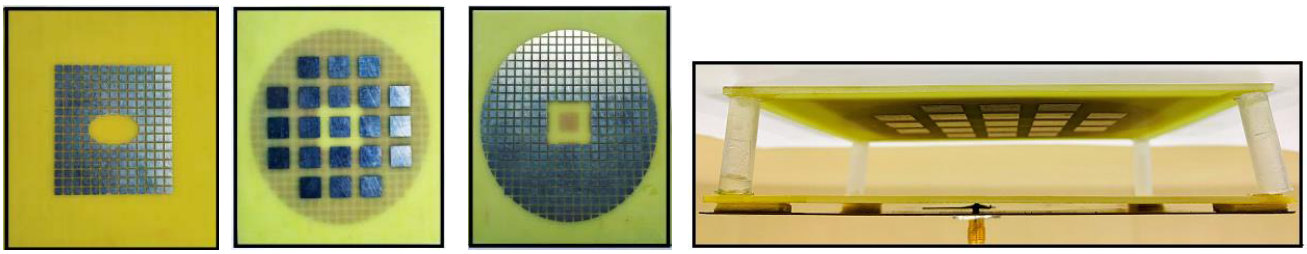

Figure 5. Photograph of prototype structure. (a) AMC-I, (b) truncated PRS, (c) AMC-II, (d) 3D view.

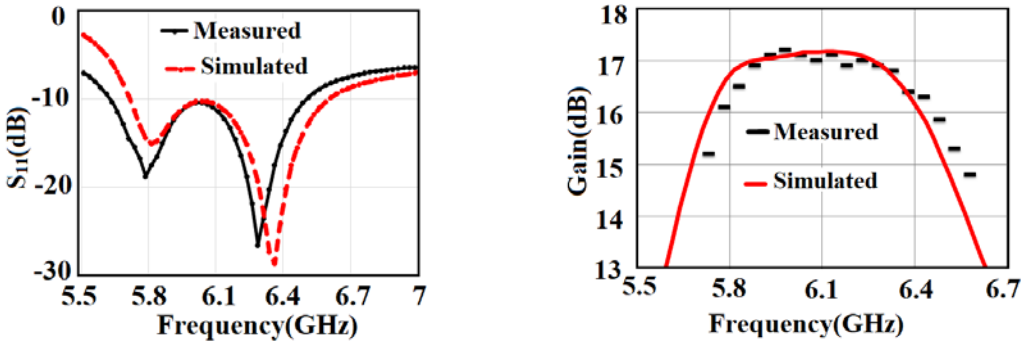

Figure 6. (a) S_{11} vs. frequency, (b) gain vs. frequency.

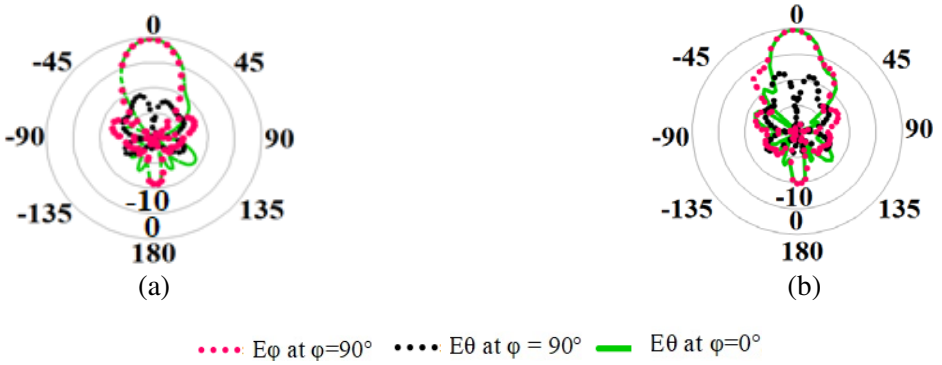

Figure 7. Radiation pattern of proposed prototype structure. (a) 5.8 GHz, (b) 6.15 GHz.

ratio BW), and the lateral size of the antenna. Therefore, the figure of merit, i.e., GBP/LA (gain BW product per unit lateral area) is calculated as shown in Table 3. Also, SLL, CPL, and profile (height) of the antenna are considered. The proposed antenna provides figure of merit 129 along with compact size $2.3\lambda_0 \times 2.75\lambda_0 \times 0.5\lambda_0$, as compared to other antennas reported in literature. The antenna structure in [5] has higher % common BW and higher figure of merit of 141; however, this antenna is $1\lambda_0$ high and suffers from high SLL (-11 dB). Reference antennas [4, 7, 8, 11, 15] have higher % common BW and more flat gain BW, but these antennas have higher SLL. Beside this, these antennas either have lower gain or larger lateral dimensions. Therefore, their GBP/LA is less than the proposed antenna. All the structures have SLL > -15 dB except [12] which has much lower figure of merit. The antenna dimensions, flat gain-frequency response, and peak gain of 17.2 dB, with gain variation < 1.2 dB over the frequency band 5.7 GHz to 6.4 GHz provide an edge to the proposed antenna over other antennas.

Table 3.

Ref.	Gain (dBi)	SLL—CPL (dB)	F/B dB	Common BW%	f_0 GHz	Size $\lambda_0 \times \lambda_0 \times \lambda_0$	GBP	GBP/LA
1	19.1	$-13\vert-22$	20	14.1	14.0	$2.9 \times 3.4 \times 0.5$	1146	116
4	13.5	$-10\vert-20$	13	32.0	10.5	$2.5 \times 2.5 \times 0.7$	716	114
5	15.0	$-11\vert-25$	NA	25.8	16.0	$2.4 \times 2.4 \times 1.3$	816	141
6	20.0	-10|NA	NA	15.0	14.5	$3.8 \times 3.8 \times 1.2$	1500	104
7	15.0	$-15\vert-20$	22	18.7	9.5	$2.3 \times 2.3 \times 0.5$	591	111
8	13.8	$-12\vert-21$	13	28.0	10.0	$2.4 \times 2.4 \times 0.5$	672	116
11	16.0	$-10\vert-15$	NA	23.0	5.5	$2.7 \times 2.7 \times 0.6$	916	121
12	17.4	$-20\vert-16$	20	11.6	5.8	$2.8 \times 3.2 \times 0.5$	637	72
13	19.4	NA|NA	NA	14.0	19.0	$4.0 \times 4.0 \times 0.5$	1219	76
15	14.0	-15|NA	NA	28.0	10.0	$2.4 \times 2.4 \times 0.5$	703	122
PA	17.2	$-19\vert-18$	20	15.2	5.8	$2.3 \times 2.7 \times 0.5$	798	129

P. A. — Proposed antenna, N. A. — Not Available, GBP — Gain BW product, GBP/LA — Gain BW product per unit lateral area.

The compact, light-weight and low-cost MSA fed FPC antenna is easy to fabricate and offers lower SLL and CPL than other reported state of art antennas.

7. CONCLUSION

In this communication, a compact, high gain, and wideband MSA using slotted elliptical and rectangular shaped AMCs and truncated PRS layer is designed, with gain variation < 1 dB over 5.725–6.4 GHz for WLAN and Satellite C band communication. The complementary AMCs and truncated PRS layers provide flat gain-frequency response and gain BW enhancement. The truncated PRS with slotted AMC layers also improves the radiation characteristics of antenna, reduces SLL and CPL, and improves F/B ratio.

REFERENCES

1. Wu, Z.-H. and W.-X. Zhang, "Broadband printed compound air fed array antennas," *IEEE Antennas Wireless Propag. Lett.*, Vol. 9, 187–191, 2010.
2. Jagtap, S., A. Chaudhari, N. Chaskar, S. Kharche, and R. K. Gupta, "A wideband microstrip array design using RIS and PRS layers," *IEEE Antennas Wireless Propag. Lett.*, Vol. 17, No. 3, 509–512, 2018.
3. Meriche, M. A., H. Attia, A. Messai, S. I. M. Sheikh, and T. A. Denidni, "Directive wideband cavity antenna with single layer metasuperstrate," *IEEE Antennas Wireless Propag. Lett.*, Vol. 18, No. 9, 1771–1774, 2019.
4. Xu, Y., R. Lian, Z. Wang, and Y.-Z. Yin, "Wideband Fabry-Perot resonator antenna with single layer partially reflective surface," *Progress In Electromagnetics Research Letters*, Vol. 65, 37–41, 2017.
5. Wang, N., Q. Liu, C. Wu, L. Talbi, Q. Zeng, and J. Xu, "Wideband Fabry-Perot resonator antenna with two layers of dielectric superstrates," *IEEE Antennas Wireless Propag. Lett.*, Vol. 14, 229–232, 2015.
6. Konstantinidis, K., A. P. Feresidis, and P. S. Hall, "Multilayer partially reflective surfaces for broadband Fabry-Perot cavity antennas," *IEEE Trans. Antennas Propag.*, Vol. 62, No. 7, 3474–3481, Jul. 2014.

7. Pirhadi, A., H. Bahrami, and J. Nasri, "Wideband high directive aperture coupled microstrip antenna design by using an FSS superstrate layer," *IEEE Trans. Antennas Propag.*, Vol. 60, No. 4, 2101–2106, 2012
8. Wang, N., Q. Liu, C. Wu, L. Talbi, Q. Zeng, and J. Xu, "Wideband Fabry-Perot resonator antenna with two complementary FSS layers," *IEEE Trans. Antennas Propag.*, Vol. 62, No. 5, 2463–2471, 2014.
9. Chen, J., Y. Zhao, Y. Ge, and L. Xing, "Dual-band high-gain Fabry Perot cavity antenna with a shared-aperture FSS layer," *IET Microw. Antennas Propag.*, Vol. 12, No. 13, 2007–2011, Oct. 2018.
10. Dang, D.-N. and C. Seo, "Compact high gain resonant cavity antenna with via hole feed patch and hybrid parasitic ring superstrate," *IEEE Access*, Vol. 7, 161963–161974, 2019.
11. Ji, L.-Y., P.-Y. Qin, and Y. J. Guo, "Wideband Fabry-Perot cavity antenna with a shaped ground plane," *IEEE Access*, Vol. 6, 2291–2297, 2018.
12. Jagtap, S. D., R. K. Gupta, N. Chaskar, S. U. Kharche, and R. Thakare, "Gain and bandwidth enhancement of circularly polarized MSA using PRS and AMC layers," *Progress In Electromagnetic Research C*, Vol. 87, 107–118, 2018.
13. Deng, F. and J. Qi, "Shrinking profile of Fabry-Perot cavity antennas with stratified metasurfaces: Accurate equivalent circuit design and broadband high-gain performance," *IEEE Antennas Wireless Propag. Lett.*, Vol. 19, No. 1, 208–212, 2020.
14. Lv, Y.-H., X. Ding, and B.-Z. Wang, "Dual-wideband high-gain Fabry-Perot cavity antenna," *IEEE Access*, Vol. 8, 4754–4760, 2020.
15. Wang, N., L. Talbi, Q. Zeng, and J. Xu, "Wideband Fabry-Perot resonator antenna with electrically thin dielectric superstrates," *IEEE Access*, Vol. 6, 14966–14973, 2018.
16. Vaid, S. and A. Mittal, "Wideband orthogonally polarized resonant cavity antenna with dual layer Jerusalem cross partially reflective surface," *Progress In Electromagnetic Research C*, Vol. 72, 105–113, 2017.
17. Xie, P. and G.-M. Wang, "Design of a frequency reconfigurable Fabry-Perot cavity antenna with single layer partially reflecting surface," *Progress In Electromagnetic Research Letters*, Vol. 70, 115–121, 2017.
18. Yadav, V., S. Bhujade, and R. K. Gupta, "Efficient high gain circularly polarized microstrip antenna using asymmetrical RIS surface," *2015 International Conference on Microwave, Optical and Communication Engineering (ICMOCE)*, 88–91, Bhubaneswar, 2015.